Article

DNA Microviscosity Characterization with Particle Diffusometry for Downstream DNA Detection Applications

Katherine Noel Clayton, Gregory D Berglund, Jacqueline C. Linnes, Tamara L. Kinzer-Ursem, and Steven T. Wereley

Anal. Chem., **Just Accepted Manuscript** • DOI: 10.1021/acs.analchem.7b03513 • Publication Date (Web): 17 Nov 2017

DNA Microviscosity Characterization with Particle Diffusometry for Downstream DNA Detection Applications

Katherine N. Clayton[1], Gregory D. Berglund[2], Jacqueline C. Linnes[2], Tamara L. Kinzer-Ursem[2*], Steven T. Wereley[1*]
1. School of Mechanical Engineering, Purdue University, West Lafayette, IN 47906
2. Weldon School of Biomedical Engineering, Purdue University, West Lafayette, IN 47906
*Author to whom correspondence should be addressed: tursem@purdue.edu, wereley@purdue.edu

Abstract

Analytical characterization of DNA microviscosity provides critical biophysical insights into nuclear crowding, nucleic acid-based pharmaceutical development, and nucleic acid-based biosensor device design. However, most viscosity characterization methods require large sample volumes and destructive testing. In contrast, particle diffusometry, permits *in situ* analysis of DNA microviscosity with short measurement times (8 seconds) using small volumes (< 3μL) which are compatible with DNA preparatory procedures. This unconventional biosensing approach involves measuring the change in sample viscosity using image processing and correlation-based algorithms. Particle diffusometry requires only a fluorescence microscope equipped with a CCD camera and is a non-destructive measurement method. We use particle diffusometry to characterize the effect of DNA topology, length, and concentration on solution viscosity. In addition, we use particle diffusometry to detect the amplification of DNA from *S. aureus* and *K. pneumoniae*, two pathogens commonly related to neonatal sepsis. Successful characterization of pathogen amplification with particle diffusometry provides a new opportunity to apply viscosity characterization toward downstream applications in nucleic acid-based pathogen detection.

Keywords: particle diffusometry, DNA viscosity, Brownian motion, isothermal amplification

Introduction

The viscous behavior of DNA suspensions provides analytical information which can be applied both in fundamental characterization of cellular responses to DNA crowding,[1] characterization of DNA binding properties,[2,3] nucleic acid drug interactions,[4] and in translational applications such as designing alternative methods for detecting nucleic acid amplification.[5] To study the viscosity of DNA, characterization is often performed with traditional measurement techniques (capillary viscometers,[6] cone-and-plate[1]). These techniques require large sample volumes (>60 μL) to perform such analyses and because they are often destructive, the sample can no longer be used in downstream applications. To address the issue of the large volumes of DNA required by existing techniques, previous researchers developed low sample volume techniques to study viscosity with methods such as microrheology,[7,8] micro-cantilever viscosity sensing,[9] and dynamic light scattering.[10] To date, much of the research involving low-volume DNA rheological analysis has focused on applications such as the influence of DNA crowding and spatial-temporal dynamics of nucleic acids in regard to cellular behavior.[11–13]

In solutions with low DNA concentrations, DNA molecules move about in an independently random fashion, and therefore the sample fluid exhibits Newtonian behavior. However, above the critical concentration (C^*) of DNA in solution, the fluid undergoes a transition from a dilute Newtonian DNA suspension to a semi-dilute, viscoelastic regime.[11] This transition to a viscoelastic fluid occurs due to DNA strand overlap, thus creating fluctuations in microviscosity due to the random motion of molecules.[14]

We characterize the fundamental properties of DNA viscosity in solutions containing DNA

above and below the critical concentration with the technique known as particle diffusometry (PD).[15–20] The solution viscosity in the presence of DNA is increased compared to the same solution without DNA (Figure 1A), and therefore in the presence of DNA particles undergo slower Brownian motion. This motion decrease can be calculated with our recently developed particle diffusometry technique. PD is a non-destructive method that provides many statistically robust viscosity measurements using correlation-based algorithms with rapid measurement times (8 sec.) to calculate an ensemble averaged solution viscosity.[16,17] This method contrasts with particle tracking techniques that follow the trajectories of individual particles in solution. Because a correlation approach is taken rather than an individual trajectory measurement, PD offers advantages in speed of measurement, shorter data acquisition times, and consequently less computational processing.[16,21,22] To measure the viscosity of DNA, PD begins by imaging 200 nm particles suspended in a 3 μL volume (Figure 1B). This small volume is essential when samples are expensive or difficult to produce and is compatible with current laboratory DNA purification procedures, such as small volume DNA purification mini-prep kits and gel extraction methods, which produce DNA solution volumes of < 20 μL.

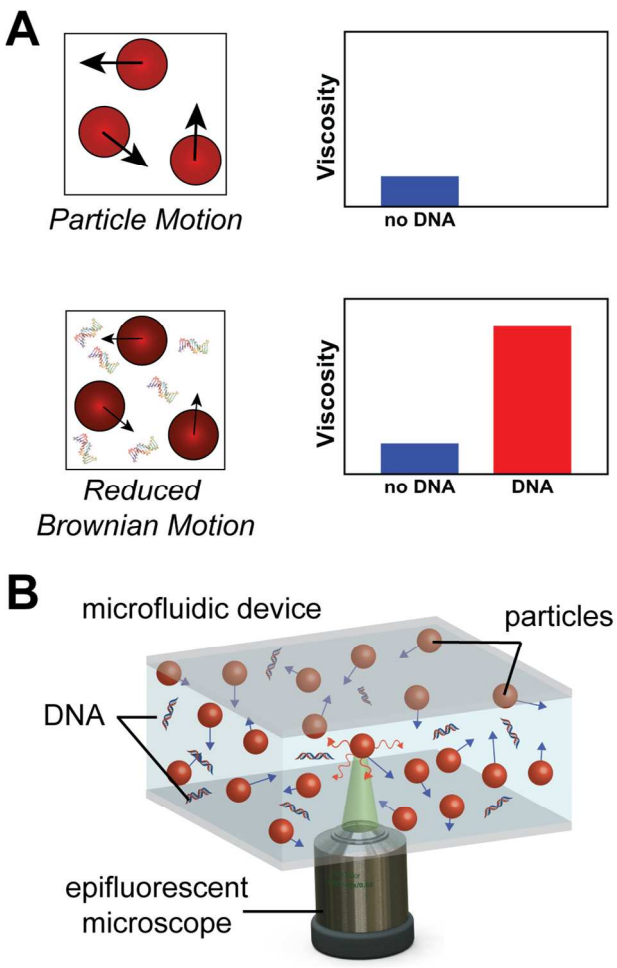

Figure 1. Measuring Viscosity for DNA Solutions. (A) Particles that are freely moving in buffer maintain an unhindered Brownian motion with low viscosity. When DNA is present in the particle solution, the Brownian motion is reduced as an effect of the increased viscosity of the solution. (B) Particle diffusometry (PD) uses microscopy to image particle motion in quiescent solutions. These measurements are made in any optically clear microfluidic chamber. In the present work, particles are imaged with an epifluorescent microscope.

In this work, we characterize how DNA length, topology, and concentration affect viscosity measurements. After extensively characterizing the effects of these DNA properties on solution viscosity, we use this information to further investigate the viscosity changes that occur when performing DNA amplification from genes present in two different pathogens, *Staphylococcus aureus* (*S. aureus*) and *Klebsiella pneumoniae* (*K. pneumoniae*). These pathogens are common

causes of neonatal sepsis, the leading cause of death in newborns worldwide.[23,24] We compare PD measurements of two different DNA amplification methods; PCR and loop-mediated isothermal amplification (LAMP). From these successful measurements, we propose the integration of nucleic acid amplification with PD as a novel method for pathogen detection.

Experimental Section

Bacteria Growth and Plasmid Purification

Chemically competent BL21(DE3) *E. coli* (New England BioLabs, Ipswich, MA) were transformed with either a 3618 bp pRSET emerald GFP (emGFP) plasmid (Invitrogen, Grand Island, NY, USA) or 6162 bp pD444-SR CaMKII lambda phosphatase plasmid (DNA 2.0, Menlo Park, CA, USA). Transformed *E. coli* were grown from 20% glycerol stocks stored at -80˚C in 5 ml Lysogeny Broth (LB) with 100 μg/ml ampicillin. The culture was maintained at 37˚C with continuous shaking at 250 rpm overnight (Forma Orbital Shaker, Thermo Electron Corporation, Waltham, MA, USA) and transferred to 1L cultures for another 5-7 hours. Plasmid DNA was then purified from *E. coli* using a QIAGEN plasmid maxi-prep kit (QIAGEN, Hilden, Germany) and stored in QIAGEN elution buffer at -20˚C. Plasmid stock concentrations were quantified using absorbance measurements at 260nm on a NanoDrop 2000 (Thermo Fisher Scientific, Waltham, MA, USA). DNA stock was diluted in elution buffer to concentrations of 0.5, 0.4, 0.3, 0.2, 0.1, 0.05, 0.025, and 0.01 mg/ml.

Linearizing DNA

To linearize plasmid DNA, restriction enzyme digests were performed on purified plasmids. Single restriction enzyme digests were performed in the plasmid DNA from the pD444-SR CaMKII lambda phosphatase (6162 bp) and pRSET emGFP (3618 bp) to linearize the entire sequence with enzymes HindIII and NdeI (New England BioLabs, Ipswich, MA), respectively.

Shorter strands of linear DNA (200 bp to 1140 bp) were synthesized using PCR in an Eppendorf Mastercycler Nexus Thermal Cycler (Eppendorf, Hamburg, Germany). For a 50 µL reaction, PCR reagents included upstream primers and downstream primers (final concentration of 0.5µM, primers listed in Table S-1) from Integrated DNA Technologies (Coralville, IA, USA), 100 ng of the appropriate DNA backbone, nuclease free water, and 25 µL of GoTaq Colorless Master Mix (Promega, Madison, WI, USA). DNA fragments of 487, 862, and 1140 bp length were amplified from the extracted and purified pD444-SR CaMKII lambda phosphatase plasmid. 200 and 250 bp DNA fragments were amplified from purified *Vibrio cholerae* (*V. cholerae*) N16961 (ATCC 39315D-5) DNA with primers designed specifically for the *ctxA* gene. We performed agarose gel electrophoresis (1.5% w/v, 100V, 1 hour, Figures S-1, S-2, and S-3) to verify either a complete restriction enzyme digestion or PCR amplification of the DNA fragments.

DNA was concentrated using ethanol precipitation and then purified using a Monarch Nucleic Acid Purification Kit (New England BioLabs, Ipswich, MA, USA). Briefly, 0.1 volumes of 3M sodium acetate and 3 volumes of 100% ethanol (stored at -20˚C) were combined with the DNA sample and left overnight at -20˚C. Samples were centrifuged at 14,000 x g at 4˚C for 30 minutes. The resulting DNA pellets were washed with chilled (-20˚C) 70% ethanol, centrifuged for another 15 minutes, and resuspended in QIAGEN elution buffer. Post-ethanol precipitation, dNTPs and polymerase were removed from DNA samples using the Monarch Nucleic Acid

Purification Kit and resuspended in the QIAGEN elution buffer. All concentrations were verified using the NanoDrop 2000.

S. aureus and K. pneumoniae DNA Extraction

Frozen stocks of *K. pneumoniae* strain BIDMC 2A and *S. aureus* strain HFH-30008 were provided by BEI Resources (Manassas, VA, USA). *K. pneumoniae* and *S. aureus* cultures were grown for approximately 24 hours in tryptic soy broth at 37°C and 280 rpm in a Fischer-Scientific Incubating Mini-Shaker. Following growth, genomic DNA was extracted from both bacteria using the commercially available QIAamp DNA Mini Kit (QIAGEN, Hilden, Germany). Extraction from *K. pneumoniae* was performed according to manufacturer instructions for the isolation of genomic DNA from Gram negative bacterial suspension cultures. Extraction from *S. aureus* followed the manufacturer instructions for the isolation from Gram positive bacteria, using 540 U of achromopeptidase in deionized water as the enzymatic solution for lysis. Prior to the addition of proteinase K, *S. aureus* was incubated with achromopeptidase solution at 37° C for 15 minutes followed by inactivation at 85°C for 2 minutes. After extraction, the genomic DNA concentration of each bacteria strain was determined using absorbance on a Nanodrop 2000.

S. aureus and K. pneumoniae PCR Amplification

PCR reactions were performed with isolated genomic DNA of both *K. pneumoniae* and *S. aureus* using GoTaq Colorless MasterMix Kit. Primers used in the reactions were chosen to correspond with LAMP reaction primers, F3 and B3 (sequence in Table S-2), based on previous studies (primers were purchased from Integrated DNA Technologies, Coralville, IA).[25,26] Three

groups of PCR reactions were run: no template DNA but with oligos that did not undergo PCR ((-) No Heat), template DNA with oligos that did not undergo PCR ((+) No Heat), and template DNA with oligos that underwent PCR ((+) Heat). All samples were made in triplicate for testing. PCR was performed following the manufacturer's protocol using 0.6 ng of template DNA for positive samples. Reactions were run using the following heating profile: 95°C initial denaturation for 2 minutes, followed by 30 cycles of: denaturing at 95°C for 30 seconds, annealing for 1 minute at 52.9°C, and extension for 40 seconds at 72°C. A final extension step was performed at 72°C for 5 minutes. Amplification was confirmed by 1.5% agarose gel electrophoresis (Figure S-4).

S. aureus and K. pneumoniae LAMP Amplification

Genomic DNA, extracted as described above, was used as the template in 25 µL LAMP reactions with reagent concentrations specified in Table S-3 in the Supplemental Information. Primers were purchased from Integrated DNA Technologies (sequences in Table S-2) and all other reagents were purchased from New England Biolabs (Ipswitch, MA, USA). Isothermal amplification was performed for 60 minutes at 65°C for each pathogen. The three conditions studied were the same as in the PCR reactions ((-) No Heat, (+) No Heat, and (+) Heat). Amplification was monitored through real-time fluorescence and further confirmed by 1.5% agarose gel electrophoresis (Figure S-5).

Particle Preparation and Dynamic Light Scattering

200 nm polystyrene particles (Fluoro-max red dyed aqueous spheres, Thermo Scientific, Erie, NY, USA) were washed three times in elution buffer (QIAGEN, Hilden, Germany) by

centrifugation at 13,000 x g for 15 minutes. Washed particles were added to the DNA samples immediately prior to imaging at a final concentration of 2.88 x 10^8 particles/mL. All DNA-particle solutions were stored at 4°C until imaging.

The nanoparticle concentration of 2.88 x 10^8 particles/mL was specifically chosen for a statistically relevant sample size while limiting the hydrodynamic interactions between particles. To ensure minimization of any particle-particle interactions that would confound our viscosity measurements, we use the relationship by Batchelor for a dilute monodisperse species of particles,

$$D_0 = D_{0*}(1 + k\phi) \quad (1)$$

where D_0 is the effective diffusion coefficient from the addition of the polystyrene spheres, D_{0*} is the diffusion coefficient of the solvent, k is the type-specific constant where we use a value of 1.45 as this value is presumed to be the most reliable from theoretical derivations,[27] and ϕ is the volume fraction of the particles in solution.[27–29] From Equation (1), the percent change in the diffusion coefficient due to the introduction of particles at a concentration of 2.88 x 10^8 particles/mL is 0.0024%. The hydrodynamic interactions of the particles may be considered negligible when this percentage is less than 0.01.[27]

Prior to measurement with PD, the diffusivity of DNA-particle samples was initially measured using dynamic light scattering (DLS) (Zetasizer Nano ZS, Malvern Instruments Ltd., United Kingdom). Standard, 70 μL disposable polystyrene cuvettes (DOT Scientific, Burton, MI, USA) were used for measurements in triplicate.

We used the Zetasizer Nano ZS to measure the Zeta potential of the 200nm polystyrene particles (DTS1060 cuvettes, Malvern Instruments Ltd., United Kingdom) to be -35$\pm$2 mV. The negative charge of these particles indicates repulsion effects when introduced to DNA solutions

(also negatively charged). Therefore, minimal-to-no adsorption of the DNA onto the particle surfaces is expected.

Particle Diffusometry Theory and Calculations

PD involves imaging the Brownian motion of particles in a solution and calculating the average particle diffusion coefficient using correlation analysis.[16] In this work we capture a series of images of 200 nm fluorescent particles undergoing Brownian motion in a quiescent volume (Figure 1B). Each image is partitioned into smaller, 64x64 pixel^2-sized interrogation areas. The size of each interrogation area is defined such that 8-10 particles, on average, are present within the interrogation area. To perform cross-correlation on the interrogation areas, we correlate a first image at time t with a second image at time $t + \Delta t$. Fundamentally, cross-correlation determines ensemble particle displacement between two sequential images (Figure 2). The larger the particle displacement during the time Δt, the broader the cross-correlation peak. The width of the peak, s_c (pixels), is determined at a height of $1/e$. Autocorrelation correlates the interrogation window at time t with itself (Figure 2). The autocorrelation peak width, s_a (also determined at a height of $1/e$), is taller and narrower when compared to the cross-correlation peak. Using this information, we calculate the diffusion coefficient using the equation derived from Olsen and Adrian:[30]

$$D = \frac{s_c^2 - s_a^2}{16 M^2 \Delta t} \quad (2)$$

where M is the magnification of the microscope objective. Because the peak width has units of pixels, using Equation (2), we can see that the squared difference in the peak widths, $s_c^2 - s_a^2$, corresponds to the change in the cross-sectional area of the correlation peak at $1/e$. By

experimentally determining the diffusion coefficient from the particle images, the Stokes-Einstein relationship can be algebraically rearranged (Equation (3)) to solve for the viscosity η of a solution.[19,31]

$$\eta = \frac{kT}{6\pi Da} \tag{3}$$

Here, k is the Boltzmann constant, T is the absolute temperature, and a is the hydrodynamic radius of the 200 nm polystyrene spheres.

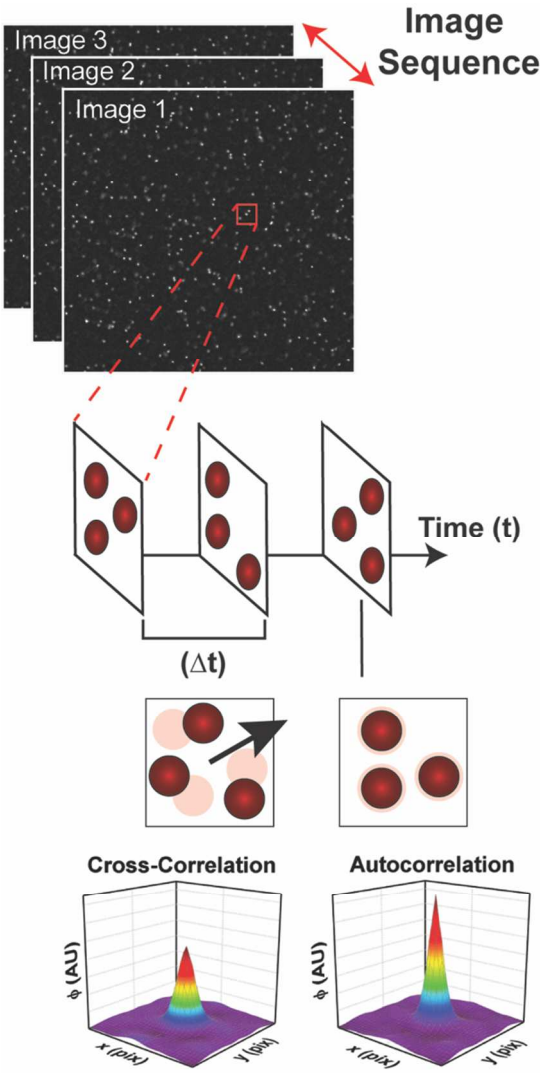

Figure 2. Particle diffusometry fundamentals. Brownian motion of 200 nm polystyrene fluorescent particles in the presence of DNA is imaged using fluorescence microscopy and recorded with a CCD camera. The sequential

image series is analyzed by splitting the image stack into smaller interrogation regions (red box). The correlation of sequential images (Image 1 with Image 2) provides the cross-correlation peak. Autocorrelation of an image with itself (for example Image 1 with Image 1) produces a taller, narrower peak relative to the cross-correlation peak.

Performing Experimental Particle Diffusometry Measurements

A fluid well to contain the DNA-particle solution was made by punching a 6 mm diameter hole (120 μm thickness) through double-sided adhesive (Therm-O-Web, Wheeling, IL, USA) which was then adhered to a cover glass slide (Thickness No. 1, Thermo Scientific, Erie, NY, USA). The 3 μL DNA-particle sample was then added to the fluid well and sealed with a second of cover glass to limit convective evaporation during imaging. Temperature was measured using a K-type thermocouple to be 21.0±0.1ºC for all DNA sample imaging.

The DNA-particle samples were imaged using an inverted fluorescence microscope (Nikon TE-2000U, Nikon, Japan) equipped with an X-cite lamp and 40X magnification objective. Images were recorded using a PCO 1600 CCD camera (PCO, Kelheim, Germany) using an 802 x 802 pixel^2 imaging window with 2 x 2 binning at 13.3 fps (Δt of 75 ms). To ensure that we negated the effects of hindered diffusion caused by the proximity of particles to any surface, we imaged particles at the mid-plane of the chip. We analyzed particles which were only located within the depth of correlation, 4.2 μm, by using an expression derived by Meinhart *et al*.[21,32] so that only particles in this location contribute significantly to the correlation function. The remainder of the particles contribute to the background signal.

Particle images were processed and auto- and cross-correlation analysis was performed using an in-house MATLAB code. The diffusion coefficient was calculated from this analysis as described in the Theory section. Nine measurements, of 100 images each, were performed for every sample. A two-dimensional Gaussian curve fit was used to calculate the orthogonal profile

of the cross- and autocorrelation peaks for both the XZ- and YZ-planes. The value of the correlation peaks (s_c and s_a) was calculated by taking the average width of the XZ- and YZ-Gaussian curves at height $1/e$.

We are interested in characterizing the effect of DNA presence on solution viscosity and not the absolute magnitude of the solution viscosity itself. Therefore, we calculate relative solution viscosity (η/η_0) by algebraic manipulation of Equation (3), where η_0 is the viscosity of the buffer solution without DNA (but still including the 200 nm polystyrene fluorescent particles):

$$\frac{\eta}{\eta_0} = \frac{D_0}{D} \quad (4)$$

PD measurements in buffer are performed to determine a baseline viscosity measurement, η_0. By calculating the relative viscosity in Equation (4), parameters such as temperature, T, and radius, a, from Equation (3) cancel out.

Results and Discussion

Plasmid DNA Viscosity

We first characterized the effect of circular plasmid DNA on solution viscosity. The relative viscosity of two different plasmids of different sizes, 3618 bp pRSET emGFP plasmid and 6162 bp pD444-SR plasmid, were measured using PD and DLS. We measured the viscosity η of DNA samples relative to QIAGEN elution buffer η_0. Therefore, all relative viscosity measurements were greater than 1. As expected, the relative viscosity of the solution steadily increased at higher DNA solution concentrations (Figures 3A and 3B, raw data in Supplementary Tables S-4 and S-5). Additionally, the longer pD444-SR plasmid showed a larger change in the relative viscosity compared to the pRSET emGFP plasmid at the higher DNA concentrations; this was seen by the steeper slope in the linear fit of the viscosity measurements of the pD444-SR plasmid

(slope of 1.22) compared to pRSET emGFP plasmid (slope of 0.88) in Figures 3A and 3B. The relative viscosity of circular pRSET emGFP and pD44-SR plasmids are plotted on the same graph in Supplementary Figure S-6A. Although both DLS and PD displayed similar trends in measured viscosity, the viscosity calculations from PD trend higher than DLS. This is likely because in DLS, properties such as refractive index and absorbance values are used in calculating the solution viscosity.[33] These assumptions may likely lead to slightly different results between DLS and PD measurements. The viscosity measurements from the two methods were highly positively correlated, with a Pearson Correlation Coefficient (R) of 0.98 (Figure 3C). Together, this data validated that PD can be used for characterizing the viscosity of DNA solutions.

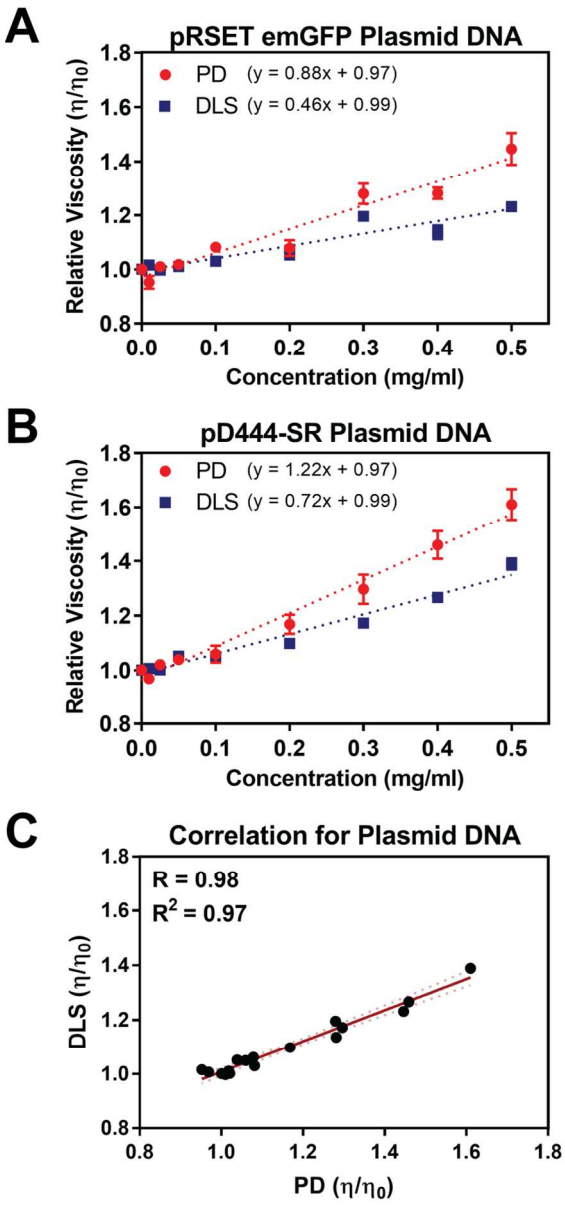

Figure 3. Changes in solution viscosity as a function of circular plasmid DNA concentration. Relative solution viscosity was measured with PD and DLS as a function of (A) increasing 3618 bp pRSET emGFP plasmid concentration and (B) increasing 6162 bp pD444-SR plasmid concentration. Measurements were relative to QIAGEN elution buffer. n = 3 independent experiments. (C) DLS and PD measurements were highly positively correlated. Pearson Correlation Coefficient = 0.98.

Linear DNA Viscosity

We were interested in characterizing the effect of different DNA lengths and concentrations on solution viscosity. The length, L, of DNA, in micrometers, is $L = 0.34 * n$ where n represents the number of kilobase pairs. The molecular weight of the solution, MW (in Daltons), is defined as $MW = n * 6.1 * 10^5$, and finally the radius of gyration, R_g, of the linear DNA is defined in Equation (5), where L_p is a persistence length of 0.5 μm.[11]

$$R_g = \left(\frac{L \cdot L_p}{3}\right)^{0.5} \quad (5)$$

Using these parameters, we calculate the critical concentration (C^*) where DNA solutions move from a dilute to semi-dilute regime (Equation (6)).[11]

$$C^* = \frac{3MW}{4\pi N_A R_g^3} \quad (6)$$

Above this concentration, the DNA acts as a viscoelastic material.[34] In this work we employed a variety of different lengths of DNA to study how physical characteristics, such as the radius of gyration and critical concentration (summarized in Table I), affect solution viscosity as characterized with PD. Using Equations (5) and (6), the physical characteristics for a range of linearized DNA base pair (bp) lengths that are experimentally studied are presented in Table I.

Table I. Physical parameters of the linearized DNA. The calculated molecular weight (MW), contour length (*L*), radius of gyration (*Rg*), and critical concentration (C*) of linearized DNA lengths ranging from 200 bp to 6162 bp.

BP Length	MW (kDa)	*L* (μm)	R_g (μm)	*C** (mg/ml)
6162	3759	2.10	0.19	0.23
3618	2207	1.23	0.14	0.30
1140	695	0.39	0.08	0.53
862	526	0.29	0.07	0.61
487	297	0.17	0.05	0.81
250	153	0.09	0.04	1.13
200	122	0.07	0.03	1.27

Using PD, we measured changes in solution viscosity as a function of increasing concentrations of linearized plasmid DNA in dilute solutions (i.e. at concentrations below the critical concentration, Table I). Similar to our analysis of circularized plasmids, we compared measurements of viscosity of linearized pD444-SR DNA to linearized pRSET emGFP DNA (Figure 4A and 4B, raw data in Supplementary Tables S-6 and S-7). As the concentration of pRSET emGFP linearized DNA increased (Figure 4A) there was a moderate increase in solution viscosity. In contrast, as the concentration of the much longer linearized pD444-SR increased, there was a larger change in the solution viscosity (Figure 4B); this again was seen by comparing the linear fit of the slopes of the relative viscosity of the linearized pRSET emGFP (slope of 1.28) and pD44-SR (slope of 3.5) in Figure 4A and 4B. The relative viscosity of linearized pRSET emGFP and pD44-SR are plotted on the same graph in Supplementary Figure S-6B. Correlation analysis between the relative viscosity measurements from PD and DLS resulted in a strong positive correlation with a Pearson Correlation Coefficient of 0.85 (Figure 4C). As the polymer chain (or DNA strand) grows longer, there are more molecule-molecule interactions (London interactions) that can occur in the solution that increase internal molecular friction, which would alter the solution microviscosity (see Equation (6)). This has been observed previously[11] and is confirmed with our findings from the PD and DLS results; the 3618 bp linear plasmid exhibited a lower relative viscosity value than the 6162 bp linear plasmid. Further, DNA topology (circular versus linearized) influenced solution viscosity with the PD and DLS measurements, where linear DNA created statistically significantly more viscous solutions than their circular plasmid counterparts. This observation agrees with what has been measured previously for linear versus circular DNA[11] and is expected because our preparation of circularized plasmid was isolated directly from *E. coli* (as opposed to ligated *in vitro* samples),

which likely contains DNA plasmids in a supercoiled confirmation, and therefore experiences fewer intermolecular forces.

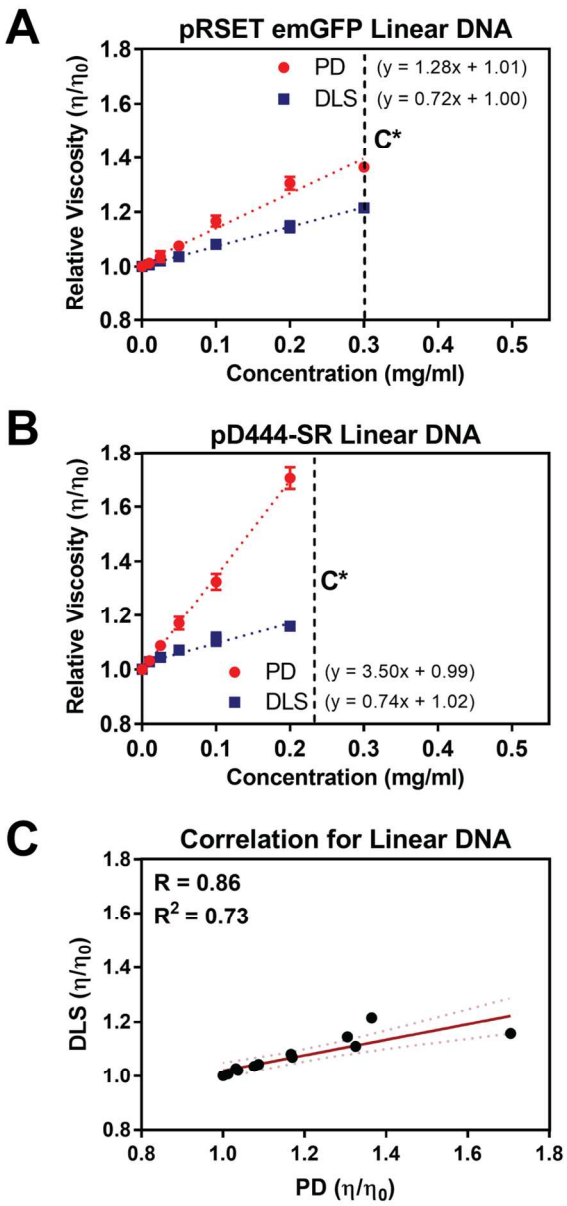

Figure 4. Changes in solution viscosity as a function of linear plasmid DNA concentration. Relative solution viscosity was measured with PD and DLS as a function of (A) increasing 3618 bp pRSET emGFP linear plasmid concentration and (B) increasing 6162 bp pD444-SR linear plasmid concentration. DNA concentrations below the critical concentration are marked by a dotted line. Measurements are relative to QIAGEN elution buffer. n = 3

independent experiments. (C) DLS and PD measurements were highly positively correlated. Pearson Correlation Coefficient = 0.85. The dashed lines indicate a 95% confidence interval.

Viscosity of Dilute and Semi-Dilute DNA Solutions

To characterize changes in DNA solution viscosity in dilute (Newtonian) and semi-dilute (viscoelastic) solutions, we used PD to measure the relative viscosity of DNA solutions at concentrations both below and above the critical concentration. Additionally, we investigated the different effects that circular and linear topology have on solution viscosity past the critical concentration value of the linear DNA (Figure 5). Having confirmed that PD measurements of viscosity are highly correlated with those from DLS, we only used PD for the remainder of our study as it is difficult to obtain the large volumes of highly concentrated DNA necessary for measurement with DLS. We observed that the linearized form of the 3618 bp pRSET emGFP DNA showed a significant increase in the viscosity at ~0.4 mg/ml (relative viscosity of 0.35 mg/ml is 1.43±0.03 and 0.4 mg/ml 2.00±0.09), which is 0.1 mg/ml greater than the theoretical critical concentration (Table I). This is further demonstrated by comparing a linear fit of the viscosity data for DNA concentrations measured below the critical concentration (Figure 5, blue dashed line, slope of 1.28) to a linear fit that includes the viscosity measurements of DNA concentrations above the critical concentration (Figure 5, orange dashed line, slope of 2.35). The difference that we see between the theoretical and experimental behavior may be due to measurement error with UV/VIS when quantifying DNA concentrations. It is notable that circular DNA did not show a sudden dramatic change in viscosity after reaching C^* (values in Supplementary Tables S-8 and linear fit in Figure 5, with a slope of 0.88). This was likely because linear DNA strands created polymer entanglement whereas circular plasmid DNA did not as easily form such entanglements,[11] and therefore did not demonstrate the same fluid

elasticity. The trends that we found in the DNA viscosity results agreed with previous literature,[9,10] further indicating that PD is a method that can reliably be used to produce viscosity measurements of DNA solutions.

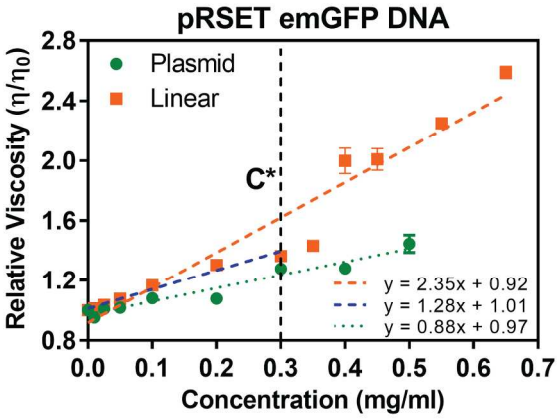

Figure 5. Viscosity of DNA solutions above the critical concentration. The effect that circular and linear DNA from the 3618 bp pRSET emGFP plasmid has on solution viscosity was compared in the dilute (C<C*) and semi-dilute (C>C*) regime. The viscosity data presented prior to 0.3 mg/ml is additionally presented in comparison with DLS measurements in Figure 3A and Figure 4A. After reaching the semi-dilute regime, the linear DNA showed a steep increase in the solution viscosity, whereas plasmid DNA showed a gradual change (n = 3). This is further demonstrated by a linear fit applied to the linear DNA viscosity measurements before critical concentration data (blue dashed line), with a slope of 2.35, and after critical concentration data is added (orange dashed line) with a slope of 1.28.

Changes in Viscosity as a Function of DNA Length and Concentration

When analyzing the viscosity of DNA in a laboratory setting, DNA fragments that encode for a specific genetic sequence will be of interest for applications in pathogen detection (short strand lengths), mutagenesis, and cloning (long DNA strand lengths). Therefore, we investigated the effects that different linear DNA strand lengths and concentrations had on solution viscosity. We examined how DNA fragments from 200 bp to 6162 bp change viscosity measurements with PD

at concentrations of 0.05, 0.1, and 0.2 mg/ml. These concentrations were chosen because PCR amplified DNA often results in concentrations within this range (values in Supplementary Table S-9). As expected, we saw that the solution viscosity of each of these fragments increased as the concentration of the DNA increased (Figure 6). Additionally, we found that longer DNA strands produced a greater change in the solution viscosity as compared to shorter DNA fragments. This is true for all concentrations measured. For example, the 6162 bp sequence had a significantly larger viscosity than a 200 bp long sequence at a concentration of 0.2 mg/ml (Figure 6A). At lower DNA concentrations, it was difficult to discern differences in relative viscosity between the larger and smaller DNA fragments (Figure 6B and 6C). Likewise, it was difficult to measure any significant difference in the viscosity of solutions with smaller DNA fragments when compared to a solution that contains no DNA whatsoever (Figure 6C).

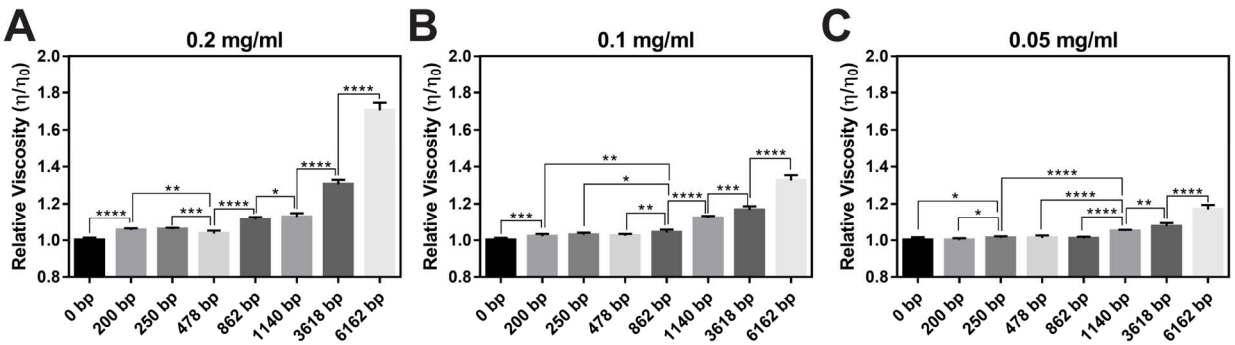

Figure 6. Effect of DNA length and concentration on solution viscosity. (A) Relative viscosity of solutions with different DNA strand lengths at 0.2 mg/ml. Statistically significant differences in relative viscosity are seen among at every ~ 200 bp. (B) Relative viscosity of solutions with different DNA strand lengths at 0.1 mg/ml at every ~ 400 bp. (C) Measurements of relative viscosity of solutions with different DNA strand lengths at 0.05 mg/ml show the least discernable changes in viscosity among the variety of DNA strand lengths at every ~ 660 bp. Only the longest 6162 bp DNA provided a statistically significant difference in solution viscosity compared to elution buffer alone (0 bp) at all three concentrations. (* $p < 0.05$, ** $p < 0.01$, *** $p < 0.001$, **** $p < 0.0001$, $n = 3$).

Detecting DNA Amplification of Blood Borne Pathogens

We used PD to measure the relative viscosity of PCR amplified samples of *S. aureus* and *K. pneumoniae* DNA. We confirmed PCR amplification (Figure S-4 and S-5) and measured the viscosity, η, of PCR samples and controls relative to QIAGEN elution buffer, η_0 with PD. Because of the added PCR buffer components, all relative viscosity measurements are greater than 1. PCR amplified *S. aureus* DNA does not show a statistically significant difference in relative viscosity compared to the control groups containing no template DNA that have not undergone the PCR temperature cycling process, nor to samples containing *S. aureus* DNA that have not undergone PCR (Figure 7A, values found in Supplementary Table S-10). The lack of measureable difference in these samples is likely due to the small length of the DNA chains that are amplified from this reaction (~200 bp) and the low concentration of end product. Furthermore, we note that the buffer used for PCR amplification (GoTaq Colorless Mastermix) contains sucrose and glycerol, both of which increase the solution viscosities relative to our previous experiments which used only elution buffer. Similar results are noted for the *K. pneumoniae* PCR amplified samples (Figure 7B), where the viscosity of the amplified end DNA product is also not statistically different relative to the control groups.

Therefore, we use PD to measure the relative viscosity of *S. aureus* and *K. pneumoniae* DNA that underwent amplification with LAMP. In Figure 7C-D, PD viscosity measurements of LAMP polymerized *S. aureus* and *K. pneumoniae* DNA show a statistically significantly higher relative viscosity compared to controls ($p < 0.0001$, $n = 3$). Similar to the PCR controls, the LAMP control groups include (1) samples that did not contain pathogen DNA and that did not undergo the LAMP heating process and (2) samples that contain template DNA but also did not undergo LAMP heating. All raw data is displayed in Table S-11. We believe that LAMP amplicons produce greater changes in viscosity as compared to PCR due to the presence of longer chain

lengths which are polymerized in the amplification process[35] (as visualized by comparing DNA bands in PCR gel in Figure S-4 to DNA bands in LAMP gel in Figure S-5). Additionally, a greater concentration of dNTPs were used in the LAMP reactions (1.4 mM) than the PCR reactions (800 μM); this likely resulted in a higher concentration of polymerized DNA in the LAMP reactions compared to the PCR reactions.

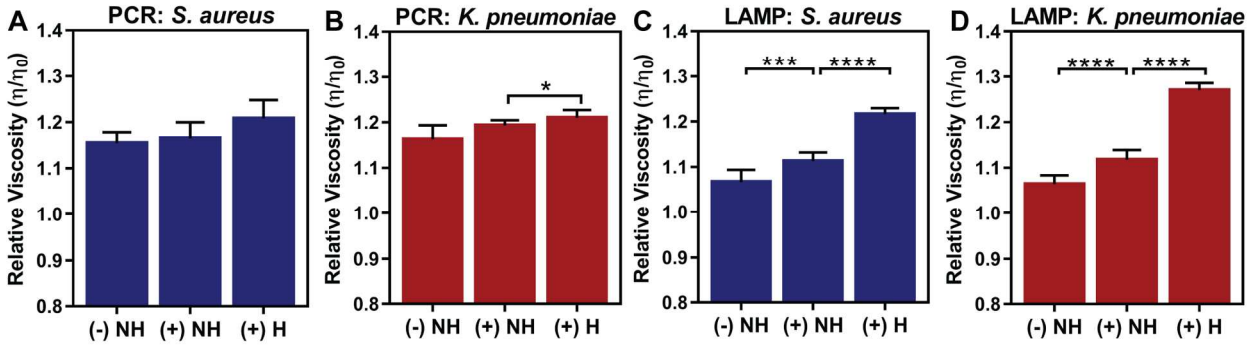

Figure 7. Relative viscosity of PCR and LAMP amplified pathogenic DNA. (A-B) PCR amplification of toxin genes from genomic (A) *S. aureus* and (B) *K. pneumoniae* DNA. (C-D) LAMP amplification of toxin genes from genomic (C) *S. aureus* and (D) *K. pneumoniae* DNA. (-) No Heat indicates samples with no genomic pathogen DNA which have not undergone the heating process used in amplification, (+) No Heat are samples with genomic DNA which have not undergone heating, and (+) Heat are samples that contained the genomic DNA which has undergone PCR or LAMP. Samples and negative controls for *S. aureus* and *K. pneumoniae* have a $\eta/\eta_0 > 1$ due to the presence of proteins and DNA primers present in the solution, altering the viscosity when relative to QIAGEN elution buffer, η_0. n = 3.

Conclusion

In this work, we demonstrate that particle diffusometry (PD) can be used to measure the viscosity of DNA-based solutions through calculating the particle diffusion coefficient in small solution volumes (< 3µL). The efficacy of PD viscosity measurements is demonstrated relative to dynamic light scattering (DLS); viscosity measurements of both methods generally agree and

are positively correlated. We further use PD to characterize the influence of concentration of linear DNA on viscosity measurements above and below the critical DNA concentration. We find that longer DNA chains indeed increase the solution viscosity relative to shorter DNA chains and that there is a significant change in solution viscosity that occurs when the DNA concentration is increased such that the solution viscosity moves from a Newtonian to viscoelastic regime (as calculated from Equation (6)) at the critical concentration. Finally, we directly apply PD to measure the viscosity of amplified DNA from the *S. aureus* and *K. pneumoniae*. We find that the viscous changes produced from a LAMP reaction are greater than from PCR due to the longer polymerized DNA chains present in the solution.

Our results show that PD is an effective method to measure the viscosity of DNA in solution, particularly when the DNA has long (> 1000 bp) chain lengths or is present at high solution concentrations. PD has advantages over current gold-standard viscosity measurements methods including the ability to make measurements in very low volumes (< 3μL). Additionally, we find that PD is a reliable method by which LAMP reactions could be characterized and as such, we foresee future applications combining the two techniques. Because the only equipment that is needed is a fluorescent microscope, a camera, and a computer, PD can be easily integrated into typical laboratory workflows and microfluidic devices. We envision that PD can be applied in measuring DNA viscosity for a broad range of research topics including pharmaceutical development, biophysical characterization, and rapid pathogen detection.

Acknowledgements

We would like to acknowledge the S.T.W., T.L.K., and J.C.L. laboratory members for the useful discussions with this work. We acknowledge the support for this work from the Purdue Office of the Executive Vice President for Research and Partnerships.

References

(1) Bravo-Anaya, L.; Pignon, F.; Martínez, F.; Rinaudo, M. *Polymers (Basel).* **2016**, *8* (8), 279.
(2) Shebl, M. *Spectrochim. Acta Part A Mol. Biomol. Spectrosc.* **2014**, *117*, 127–137.
(3) Mal, S. K.; Chattopadhyay, T.; Fathima, A.; Purohit, C. S.; Kiran, M. S.; Nair, B. U.; Ghosh, R. *Polyhedron* **2017**, *126*, 23–27.
(4) Patel, M. N.; Chhasatia, M. R.; Patel, S. H.; Bariya, H. S.; Thakkar, V. R. *J. Enzyme Inhib. Med. Chem.* **2009**, *24* (3), 715–721.
(5) Curtin, D. M.; Newport, D. T.; Davies, M. R. *Exp. Therm. Fluid Sci.* **2006**, *30* (8), 843–852.
(6) Harding, S. E. *Prog. Biophys. molec. Biol.* **1997**, *68* (23), 207–262.
(7) Apgar, J.; Tseng, Y.; Fedorov, E.; Herwig, M. B.; Almo, S. C.; Wirtz, D. *Biophys. J.* **2000**, *79* (2), 1095–1106.
(8) Bloom, R. J.; George, J. P.; Celedon, A.; Sun, S. X.; Wirtz, D. *Biophys. J.* **2008**, *95* (8), 4077–4088.
(9) Rust, P.; Cereghetti, D.; Dual, J. *Lab Chip* **2013**, *13* (24), 4794–4799.
(10) Gilroy, E. L.; Hicks, M. R.; Smith, D. J.; Rodger, A. *Analyst* **2011**, *136* (20), 4159.
(11) Goodman, A.; Tseng, Y.; Wirtz, D. *J. Mol. Biol.* **2002**, *323*, 199–215.
(12) Wang, Y. L.; Silverman, J. D.; Cao, L. G. *J. Cell Biol.* **1994**, *127* (4), 963–971.
(13) Bacher, C. P.; Reichenzeller, M.; Athale, C.; Herrmann, H.; Eils, R. *BMC Cell Biol.* **2004**, *5*, 45.
(14) Zhu, X.; Kundukad, B.; Van Der Maarel, J. R. C. *J. Chem. Phys.* **2008**, *129* (18), 1–6.
(15) Gorti, V. M.; Shang, H.; Wereley, S. T.; Lee, G. U. *Langmuir* **2008**, *24* (6), 2947–2952.
(16) Clayton, K. N.; Salameh, J. W.; Wereley, S. T.; Kinzer-Ursem, T. L. *Biomicrofluidics* **2016**, *10* (5), 1–15.
(17) Clayton, K. N.; Lee, D. H.; Wereley, S. T.; Kinzer-Ursem, T. L. *Lab Chip* **2017**.
(18) Chamarthy, P.; Garimella, S. V.; Wereley, S. T. *Exp. Fluids* **2009**, *47* (1), 159–170.
(19) Chuang, H.-S.; Sie, Y.-S. *Microfluid. Nanofluidics* **2014**, *16*, 65–72.
(20) Wereley, S.; Hohreiter, V.; Chung, J. *Therm. Challenges Next Gener. Electron. Syst.* **2002**, 95–102\r404.
(21) Raffel, M.; Willert, C. E.; Wereley, S. T.; Kompenhans, J. *Particle Image Velocimetry: A Practical Guide*; 2007; Vol. 2nd.
(22) Chamarthy, P.; Wereley, S. T. In *Encyclopedia of Nanotechnology*; Springer US, 2008; pp 1300–1305.

(23) Stoll, B. J. *Pediatrics* **2016**, *138* (6), 2013–2017.
(24) Verma, P.; Berwal, P. K.; Nagaraj, N.; Swami, S.; Jivaji, P.; Narayan, S. *Int. J. Contemp. Pediatr. Vol 2, No 3 July-September 2015* **2017**.
(25) Kinoshita, Y.; Niwa, H.; Katayama, Y. *Microbiology and Immunology*. 2015, pp 365–370.
(26) Zhao, X.; Li, Y.; Park, M.; Wang, J.; Zhang, Y.; He, X.; Forghani, F.; Wang, L.; Yu, G.; Oh, D. H. *J. Microbiol. Biotechnol.* **2013**, *23* (2), 246–250.
(27) Elimelech, M.; Gregory, J.; Jia, X.; Williams, R. In *Particle Deposition & Aggregation: Measurement, Modelling and Simulation*; Butterworth–Heinemann, 1998; pp 93–96.
(28) Batchelor, G. K. *J. Fluid Mech.* **1977**, *83* (1), 97.
(29) Batchelor, G. K. *J. Fluid Mech.* **1976**, *74* (1), 1.
(30) Olsen, M. G.; Adrian, R. J. *Exp. Fluids* **2000**, *29*, S166–S174.
(31) Einstein, A. *Ann. Phys.* **1905**, *17*, 549.
(32) Meinhart, C. D.; Wereley, S. T.; Gray, M. H. B. *Meas. Sci. Technol.* **2000**, *11* (6), 809–814.
(33) Koppel, D. E. *J. Chem. Phys.* **1972**, *57* (11), 4814–4820.
(34) Lee, J.; Tripathi, A. *Anal. Chem.* **2005**, *77* (22), 7137–7147.
(35) Notomi, T. *Nucleic Acids Res.* **2000**, *28* (12), 63e–63.

For Table of Contents Only

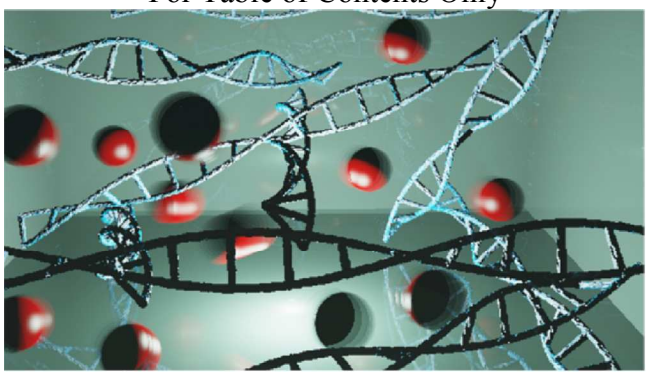

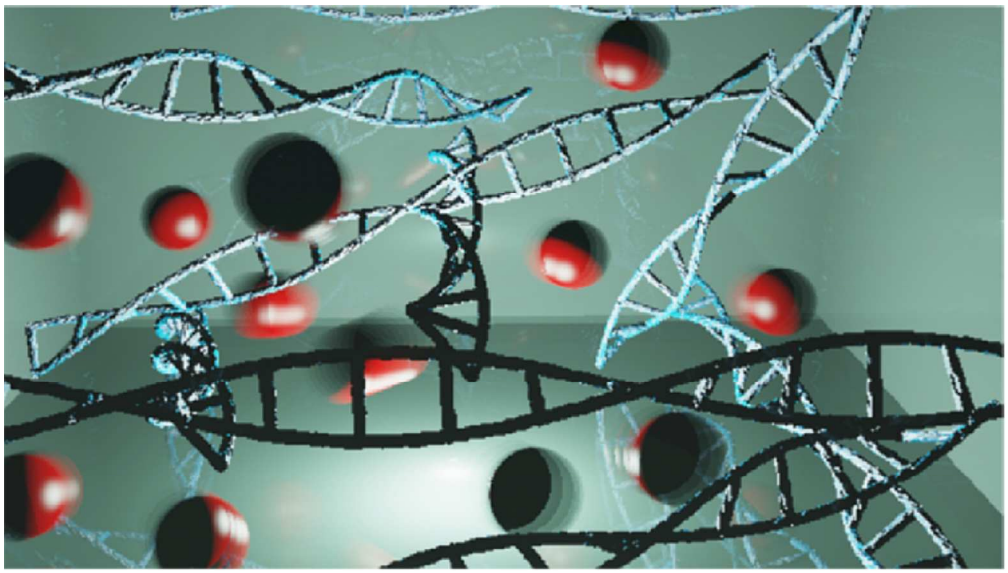

84x47mm (300 x 300 DPI)